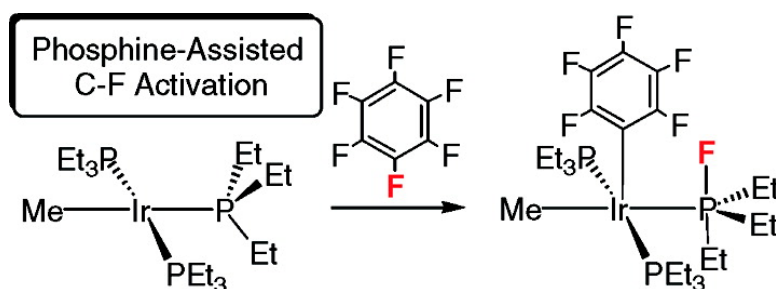


Computational Study of the Reaction of CF with [IrMe(PEt)]: Identification of a Phosphine-Assisted C#F Activation Pathway via a Metallophosphorane Intermediate

Stefan Erhardt, and Stuart A. Macgregor

J. Am. Chem. Soc., **2008**, 130 (46), 15490-15498 • DOI: 10.1021/ja804622j • Publication Date (Web): 25 October 2008

Downloaded from <http://pubs.acs.org> on February 8, 2009



More About This Article

Additional resources and features associated with this article are available within the HTML version:

- Supporting Information
- Links to the 1 articles that cite this article, as of the time of this article download
- Access to high resolution figures
- Links to articles and content related to this article
- Copyright permission to reproduce figures and/or text from this article

[View the Full Text HTML](#)

Computational Study of the Reaction of C₆F₆ with [IrMe(PET₃)₃]: Identification of a Phosphine-Assisted C–F Activation Pathway via a Metallophosphorane Intermediate

Stefan Erhardt and Stuart A. Macgregor*

School of Engineering and Physical Sciences, Heriot-Watt University,
Edinburgh EH14 4AS, U.K.

Received June 24, 2008; E-mail: s.a.macgregor@hw.ac.uk

Abstract: Density functional theory calculations have been used to model the reaction of C₆F₆ with [IrMe(PET₃)₃], which proceeds with both C–F and P–C bond activation to yield *trans*-[Ir(C₆F₅)(PEt₃)₂(PEt₂F)], C₂H₄, and CH₄ (Blum, O.; Frolow, F.; Milstein, D. *J. Chem. Soc., Chem. Commun.* **1991**, 258). Using a model species, *trans*-[IrMe(PH₃)₂(PH₂Et)], a low-energy mechanism involving nucleophilic attack of the electron-rich Ir metal center at C₆F₆ with displacement of fluoride has been identified. A novel feature of this process is the capture of fluoride by a phosphine ligand to generate a metallophosphorane intermediate [Ir(C₆F₅)(Me)(PH₃)₂(PH₂EtF)]. These events occur in a single step via a 4-centered transition state, in a process that we have termed “phosphine-assisted C–F activation”. Alternative mechanisms based on C–F activation via concerted oxidative addition or electron-transfer processes proved less favorable. From the metallophosphorane intermediate the formation of the final products can be accounted for by facile ethyl group transfer from phosphorus to iridium followed by β-H elimination of ethene and reductive elimination of methane. The interpretation of phosphine-assisted C–F activation in terms of nucleophilic attack is supported by the reduced activation barriers computed with the more electron-rich model reactant *trans*-[IrMe(PMe₃)₂(PMe₂Et)] and the higher barriers found with lesser fluorinated arenes. Reactivity patterns for a range of fluoroarenes indicate the dominance of the presence of ortho-F substituents in promoting phosphine-assisted C–F activation, and an analysis of the charge distribution and transition state geometries indicates that this process is controlled by the strength of the Ir-aryl bond that is being formed.

Introduction

The activation of C–F bonds by transition metal centers continues to receive much attention, and the fundamental understanding of this process is now maturing into practical application.¹ Thus C–F bond activation offers new routes to metal–fluoride complexes under mild conditions² and also reveals potential new routes to fluorinated organics including species that are hard to access by conventional reactions. Often, such strategies work by selective defluorination of polyfluorinated molecules, rather than by selective fluorination. Homogeneous catalytic reactions of fluoroaromatics² now encompass cross-coupling³ and hydrodefluorination processes.⁴ C–F bond activation reactions may form metal–fluoroaryl complexes that exhibit interesting reactivity, most notably [1,3]-fluorine-to-metal shifts and β-abstraction of a fluoride.⁵ The enormous range of

fluorinated drugs and fluorinated materials now in use emphasizes the scope for practical applications.⁶

As C–F activation advances, several different classes of reaction product and mechanistic possibilities have become apparent. The field has been treated systematically by reaction type in a recent review,^{2a} where the following classes of

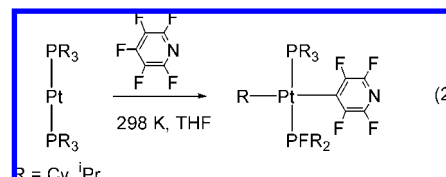
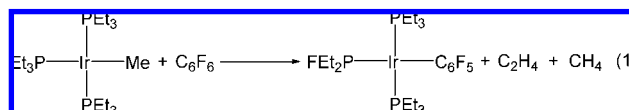
- (1) For reviews see: (a) Kiplinger, J. L.; Richmond, T. G.; Osterberg, C. E. *Chem. Rev.* **1994**, *94*, 373. (b) Burdeniuc, J.; Jedlicka, B.; Crabtree, R. H. *Chem. Ber.* **1997**, *130*, 145. (c) Murphy, E. F.; Murugavel, R.; Roesky, H. W. *Chem. Rev.* **1997**, *97*, 3425. (d) Torrens, H. *Coord. Chem. Rev.* **2005**, *249*, 1957. (e) Jones, W. D. *Dalton Trans.* **2003**, 3991.
- (2) (a) Braun, T.; Perutz, R. N. Transition-Metal Mediated C-F Bond Activation. In *Comprehensive Organometallic Chemistry III*; Crabtree, R. H., ; Mingos, D. M. P., Eds.; Elsevier: Amsterdam, 2006. (b) Braun, T.; Perutz, R. N. *Chem. Commun.* **2002**, 2749.

- (3) (a) Kiso, Y.; Tamao, K.; Kumada, M. *J. Organomet. Chem.* **1973**, *50*, C12. (b) Aizenberg, M.; Milstein, D. *Science* **1994**, *265*, 359. (c) Ishii, Y.; Chatani, N.; Yorimitsu, S.; Murai, S. *Chem. Lett.* **1998**, 157. (d) Young, R. J., Jr.; Grushin, V. V. *Organometallics* **1999**, *18*, 294. (e) Yang, H.; Gao, H. R.; Angelici, R. J. *Organometallics* **1999**, *18*, 2285. (f) Widdowson, D. A.; Wilhelm, R. E. *Chem. Commun.* **1999**, 2211. (g) Wilhelm, R.; Widdowson, D. A. *J. Chem. Soc., Perkin Trans. I* **2000**, 3808. (h) Böhm, V. P. W.; Gstöttmayr, C. W. K.; Weskamp, T.; Herrmann, W. A. *Angew. Chem., Int. Ed.* **2001**, *40*, 3387. (i) Braun, T.; Perutz, R. N.; Sladek, M. I. *Chem. Commun.* **2001**, 2254–2255. (j) Mongin, F.; Mojovic, L.; Guillamet, B.; Trecourt, F.; Queguiner, G. *J. Org. Chem.* **2002**, *67*, 8991. (k) Kuhl, S.; Schneider, R.; Fort, Y. *Adv. Synth. Catal.* **2003**, *345*, 341. (l) Widdowson, D. A.; Wilhelm, R. *Chem. Commun.* **2003**, 578. (m) Terao, J.; Ikumi, A.; Kuniyasu, H.; Kambe, N. *J. Am. Chem. Soc.* **2003**, *125*, 5646. (n) Lamm, K.; Stollenz, M.; Meier, M.; Görls, H.; Walther, D. *J. Organomet. Chem.* **2003**, *681*, 24. (o) Dankwardt, J. W. *J. Organomet. Chem.* **2005**, *690*, 932. (p) Saeki, T.; Takashima, Y.; Tamao, K. *Synlett* **2005**, *11*, 1771. (q) Steffen, A.; Sladek, M. I.; Braun, T.; Neumann, B.; Stämmler, H.-G. *Organometallics* **2005**, *24*, 4057. (r) Ackermann, L.; Born, R.; Spatz, J. H.; Meyer, D. *Angew. Chem., Int. Ed.* **2005**, *44*, 7216. (s) Yoshikai, N.; Mashima, H.; Nakamura, E. *J. Am. Chem. Soc.* **2005**, *127*, 17978. (t) Guo, H.; Kong, F.; Kanno, K.-I.; He, J.; Nakajima, K.; Takahashi, T. *Organometallics* **2006**, *25*, 2045. (u) Schaub, T.; Backes, M.; Radius, U. *J. Am. Chem. Soc.* **2006**, *128*, 15964. (v) Braun, T.; Wehmeier, F.; Altenhöner, K. *Angew. Chem., Int. Ed.* **2007**, *46*, 5321.

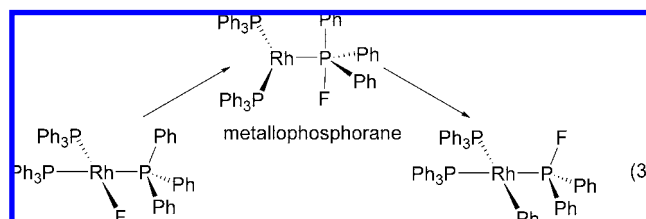
stoichiometric intermolecular reactions of fluoroaromatics were identified: (1) oxidative addition, (2) M–C bond formation with H–F elimination, (3) M–C bond formation with fluorosilane elimination, (4) hydrodefluorination with M–F bond formation, and (5) nucleophilic attack. For perfluorinated aromatics, examples of intermolecular C–F activation at low-valent late transition metal centers are known with net oxidative addition (often via η^2 -arene intermediates),⁷ as well as with HF^{8a,9} or fluorosilane⁴ elimination. The nucleophilic attack of electron-rich organometallics at perfluorinated aromatics has been recognized since the 1960s.¹⁰ C–F activation can be induced photochemically,^{8,9c} whereas the electron-deficient nature of fluorinated substrates means that electron-transfer processes may also be possible.^{9b} The factors controlling the oxidative addition of aromatic C–F bonds at late transition metal centers has also been studied computationally,¹¹ while a range of different aromatic C–F bond activation processes have been considered for lanthanide species.¹²

In addition to these possibilities, in recent years a new class of intermolecular aromatic C–F bond activation occurring with metal–phosphine complexes has begun to emerge. These novel reactions yield M–aryl products, but without the anticipated formation of a metal–fluoride bond. Instead, fluorine is transferred to a phosphorus center and displaces one of the original phosphine substituents to generate a fluorophosphine ligand in the product. The first example of this type of reactivity

was reported by Milstein and co-workers in 1991.¹³ Upon heating [IrMe(PEt₃)₃] in C₆F₆ at 60 °C cleavage of a C–F bond and formation of the fluorophosphine complex, *trans*-[Ir(C₆F₅)(PEt₃)₂(PEt₂F)], was observed. The displaced ethyl moiety presumably plays a role in the formation of ethene and methane (eq 1). At the time a C–F bond activation mechanism involving electron transfer was proposed on the basis of the selectivity of this process for C₆F₆: at 60 °C, no reaction was seen with benzene, fluorobenzene, or 1,3,5-trifluorobenzene.



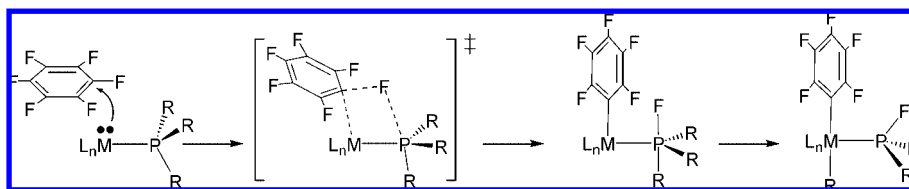
More recently, Perutz and co-workers reported that the room temperature reaction of [Pt(PR₃)₂] (R = Cy, *i*Pr) with pentafluoropyridine in THF yields fluorophosphine complexes of the type [Pt(4-C₅NF₄)(R)(PR₃)(PR₂F)].¹⁴ In this case the alkyl substituent remains intact and is transferred to the metal center (eq 2). Grushin subsequently reported similar trends in the reactions of [Pt(PCy₃)₂] with C₆F₆.¹⁵ The above examples involve intermolecular C–F bond activation; however, in some cases fluorophosphine ligands have also been produced from the reactions of metal–fluoride complexes.^{16,17} Such M–F/P–R exchange reactions have also been recently reviewed.¹⁸ The best characterized example has been reported by Grushin and Marshall who showed that heating [RhF(PPh₃)₃] in benzene led to F/Ph exchange to produce the fluorophosphine complex *cis*-[Rh(Ph)(PPh₃)₂(PPh₂F)].^{15,16} Subsequent density functional theory (DFT) calculations established that F/Ph exchange in this system occurred via a metallophosphorane intermediate characterized by initial transfer of the fluoride ligand onto a *cis* phosphine (eq 3).¹⁹ The energetic accessibility of metallophosphoranes in this, as well as other related processes²⁰ led Grushin¹⁵ to propose that such species may also be involved in



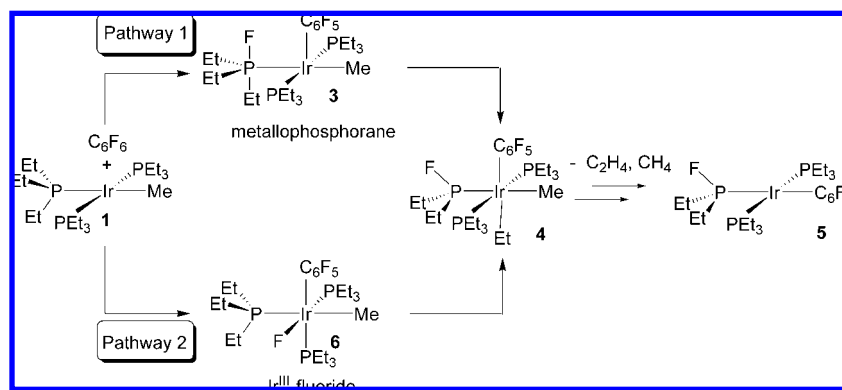
- (4) (a) Aizenberg, M.; Milstein, D. *Science* **1994**, *265*, 359. (b) Aizenberg, M.; Milstein, D. *J. Am. Chem. Soc.* **1995**, *117*, 8674. (c) Vela, J.; Smith, J. M.; Yu, Y.; Ketterer, N. A.; Flaschenriem, C. J.; Lachicotte, R. J.; Holland, P. L. *J. Am. Chem. Soc.* **2005**, *127*, 7857.
- (5) (a) Kraft, B. M.; Lachicotte, R. J.; Jones, W. D. *Organometallics* **2002**, *21*, 727. (b) Hughes, R. P.; Williamson, A.; Sommer, R. D.; Rheingold, A. L. *J. Am. Chem. Soc.* **2001**, *123*, 7443. (c) Hughes, R. P.; Laritchev, R. B.; Williamson, A.; Incarvito, C. D.; Zakharov, L. N.; Rheingold, A. L. *Organometallics* **2002**, *21*, 4873.
- (6) Müller, K.; Faeh, C.; Diederich, F. *Science* **2007**, *317*, 1881.
- (7) (a) Fahey, D. R.; Mahan, J. E. *J. Am. Chem. Soc.* **1977**, *99*, 2501. (b) Hofmann, P.; Unfried, G. *Chem. Ber.* **1992**, *125*, 659. (c) Belt, S. T.; Helliwell, M.; Jones, W. D.; Partridge, M. G.; Perutz, R. N. *J. Am. Chem. Soc.* **1993**, *115*, 1429. (d) Bach, I.; Pörschke, K. R.; Goddard, R.; Kopske, C.; Krüger, C.; Rufinska, A.; Seevogel, K. *Organometallics* **1996**, *15*, 4959. (e) Cronin, L.; Higgitt, C. L.; Karch, R.; Perutz, R. N. *Organometallics* **1997**, *16*, 4920. (f) Yamamoto, T.; Abila, M. *J. Organomet. Chem.* **1997**, *535*, 209. (g) Braun, T.; Cronin, L.; Higgitt, C. L.; McGrady, J. E.; Perutz, R. N.; Reinhold, M. *New J. Chem.* **2001**, *25*, 19. (h) Schaub, T.; Radius, U. *Chem.–Eur. J.* **2005**, *11*, 5024.
- (8) (a) Belt, S. T.; Duckett, S. B.; Helliwell, M.; Perutz, R. N. *J. Chem. Soc., Chem. Commun.* **1989**, 928. (b) Jones, W. D.; Partridge, M. G.; Perutz, R. N. *J. Chem. Soc., Chem. Commun.* **1991**, 266.
- (9) (a) Klahn, A. H.; Moore, M. H.; Perutz, R. N. *J. Chem. Soc., Chem. Commun.* **1992**, 1699. (b) Whittlesey, M. K.; Perutz, R. N.; Moore, M. H. *Chem. Commun.* **1996**, 787. (c) Klahn, A. H.; Oelckers, B.; Godoy, F.; Garland, M. T.; Vega, A.; Perutz, R. N.; Higgitt, C. L. *J. Chem. Soc., Dalton Trans.* **1998**, 3079. (d) Jasim, N. A.; Perutz, R. N. *J. Am. Chem. Soc.* **2000**, *122*, 8685.
- (10) (a) King, R. B.; Bisnette, M. B. *J. Organomet. Chem.* **1964**, *2*, 38. (b) Bruce, M. I.; Stone, F. G. A. *J. Chem. Soc. A.* **1966**, 1837. (c) Artamkina, G. A.; Mil'chenko, A. Y.; Beletskaya, I. P.; Reutov, O. A. *J. Organomet. Chem.* **1986**, *311*, 199. (d) Edelbach, B. L.; Jones, W. D. *J. Am. Chem. Soc.* **1997**, *119*, 7734. (e) Peterson, T. H.; Golden, J. T.; Bergman, R. G. *Organometallics* **1999**, *18*, 2005.
- (11) (a) Bosque, R.; Clot, E.; Fantacci, S.; Maseras, F.; Eisenstein, O.; Perutz, R. N.; Renkema, K. B.; Caulton, K. G. *J. Am. Chem. Soc.* **1998**, *120*, 12634. (b) Jakt, M.; Johannissen, L.; Rzepa, H. S.; Widdowson, D. A.; Wilhelm, R. *J. Chem. Soc., Perkin Trans. 2* **2002**, 576. (c) Reinhold, M.; McGrady, J. E.; Perutz, R. N. *J. Am. Chem. Soc.* **2004**, *126*, 5268. (d) Bahmanyar, S.; Borer, B. C.; Kim, Y. M.; Kurtz, D. M.; Yu, S. *Org. Lett.* **2005**, *7*, 1011.
- (12) Maron, L.; Werkema, E. L.; Perrin, L.; Eisenstein, O.; Andersen, R. A. *J. Am. Chem. Soc.* **2005**, *127*, 279.

- (13) Blum, O.; Frolow, F.; Milstein, D. *J. Chem. Soc., Chem. Commun.* **1991**, 258.
- (14) Jasim, N. A.; Perutz, R. N.; Whitwood, A. C.; Braun, T.; Izundu, J.; Neumann, B.; Rothfeld, S.; Stammler, H. G. *Organometallics* **2004**, *23*, 6140.
- (15) Macgregor, S. A.; Roe, D. C.; Marshall, W. J.; Bloch, K. M.; Bakhmutov, V. I.; Grushin, V. V. *J. Am. Chem. Soc.* **2005**, *127*, 15304.
- (16) Grushin, V. V.; Marshall, W. J. *J. Am. Chem. Soc.* **2004**, *126*, 3068.
- (17) Geldbach, T. J.; Pregosin, P. S. *Eur. J. Inorg. Chem.* **2002**, 1907, and references therein.
- (18) Macgregor, S. A. *Chem. Soc. Rev.* **2007**, *36*, 67.
- (19) Macgregor, S. A.; Wondimagegn, T. *Organometallics* **2007**, *26*, 1143.

Scheme 1



Scheme 2



the unusual C–F bond activation chemistry observed with $[\text{IrMe}(\text{PEt}_3)_3]$ and $[\text{Pt}(\text{PR}_3)_2]$ (see Scheme 1). Nucleophilic attack of an electron-rich metal at a fluoroaromatic would lead to C–F bond cleavage. If this occurred with trapping of the displaced fluoride by an adjacent phosphine ligand, a metallophosphorane intermediate would be formed. Subsequent transfer of one substituent, R, from phosphorus to the metal center would then complete fluorophosphine formation.

In this and the accompanying paper on group 10 *bis*-trialkylphosphine Pt(0) species²¹ we present the results of DFT calculations to test the above hypothesis. In both cases, C–F activation via a metallophosphorane species accounts for the observed formation of fluorophosphine complexes. A new pathway for intermolecular C–F bond activation has therefore been identified that we have termed “phosphine-assisted C–F activation”. This novel mechanism is a further case where metallophosphoranes play a central role in organometallic reactivity.^{15,18–20,22}

Computational Details

All DFT calculations were run with Gaussian 03^{23a} using the BP86 functional.^{23b–g} For the small-model calculations derived from *trans*- $[\text{Ir}(\text{Me})(\text{PH}_3)_2(\text{PH}_2\text{Et})]$, **1'**. The SSD pseudopotential and the associated basis set were used to describe Ir,^{24a} 6-31G** basis sets were used for all other atoms.²⁵ With the larger model *trans*-

$[\text{Ir}(\text{Me})(\text{PMe}_3)_2(\text{PMe}_2\text{Et})]$, **1'** (**PMe**₃), P was described with the SDD pseudopotential and associated basis set, augmented by a set of d-orbital polarization functions ($\zeta = 0.387$),^{24b} and 6-31G basis sets were employed for phosphine methyl substituents. All stationary points were fully characterized via analytical frequency calculations as either minima (all positive eigenvalues) or transition states (one imaginary eigenvalue), and IRC calculations were used to confirm the minima linked by each transition state. Reported energies include a correction for zero-point energies, and free energies are at 298.15 K. The effects of solvent polarity on the energetics of the various C–F bond activation mechanism were tested via PCM calculations (C_6H_6 , $\epsilon = 2.25$) and shown to be minimal.

Results and Discussion

The basis of our computational modeling of the reaction of $[\text{IrMe}(\text{PEt}_3)_3]$ with C_6F_6 is shown in Scheme 2. The major challenge is to define the mechanism by which an ethyl complex such as **4** is formed. This species has the pentafluoroaryl and fluorophosphine ligands of the ultimate product *trans*- $[\text{Ir}(\text{C}_6\text{F}_5)(\text{PEt}_3)_2(\text{PEt}_2\text{F})]$ (**5**) in place, and a simple route converting **4** to **5** can be envisaged via β -H elimination of ethene and reductive elimination of methane. We will consider two pathways for the formation of **4** which differ in their mode of C–F activation. In Pathway 1, phosphine-assisted C–F activation produces metallophosphorane intermediate **3** from which Et group transfer from P to Ir generates **4**. Alternatively, Pathway 2 proceeds via oxidative addition of C_6F_6 to **1** to give an Ir^{III}–fluoride such as **6**. F/Et exchange in **6** (analogous to the F/Ph exchange observed with $[\text{RhF}(\text{PPh}_3)_3]$)^{15,19} would then give **4**. These possibilities have been explored with calculations on the model system *trans*- $[\text{Ir}(\text{Me})(\text{PH}_3)_2(\text{PH}_2\text{Et})]$, **1'**. In practice, Pathways 1 and 2 can be distinguished by the ease of the C–F activation steps involved, and these will be discussed in

- (20) Macgregor, S. A.; Neave, G. W. *Organometallics* **2004**, *23*, 891.
 (21) Flores, A. N.; Erhardt, S.; Jasim, N.; Perutz, R. N.; Macgregor, S. A.; McGrady, J. E.; Whitwood, A. C. *J. Am. Chem. Soc.* **2008**, *130*, 15499.
 (22) (a) For reviews of metallophosphorane chemistry see: Dillon, K. B. *Chem. Rev.* **1994**, *94*, 1441. (b) Nakazawa, H.; Kubo, K.; Miyoshi, K. *Bull. Chem. Soc. Jpn.* **2001**, *74*, 2255. (c) Other examples: Vierling, P.; Riess, J. G. *Organometallics* **1986**, *5*, 2543, and references therein. (d) Kajiyama, K.; Nakamoto, A.; Miyazawa, S.; Miyamoto, T. K. *Chem. Lett.* **2003**, *32*, 332. (e) Braga, A. A. C.; Morgon, N. H.; Ujaque, G.; Maseras, F. *J. Am. Chem. Soc.* **2005**, *127*, 9298.
 (23) (a) Frisch, M. J.; et al. *Gaussian 03*, revision C.02; Gaussian, Inc.: Wallingford CT, 2004. (b) Becke, A. D. *Phys. Rev. A* **1998**, *38*, 3098. (c) Becke, A. D. *J. Chem. Phys.* **1993**, *98*, 1372. (d) Becke, A. D. *J. Chem. Phys.* **1993**, *98*, 5648. (e) Vosko, S. H.; Wilk, L.; Nusair, M. *Can. J. Phys.* **1980**, *58*, 1200. (f) Becke, A. D. *J. Chem. Phys.* **1986**, *84*, 4524. (g) Perdew, J. P. *Phys. Rev. B* **1986**, *33*, 8822.

- (24) (a) Andrae, D.; Häusserman, U.; Dolg, M.; Stoll, H.; Preuss, H. *Theor. Chim. Acta* **1990**, *77*, 123. (b) Höllwarth, A.; Böhme, M.; Dapprich, S.; Ehlers, A. W.; Gobbi, A.; Jonas, V.; Köhler, K. F.; Stegmann, R.; Veldkamp, A.; Frenking, B. *Chem. Phys. Lett.* **1993**, *208*, 237.
 (25) (a) Hehre, W. J.; Ditchfield, R.; Pople, J. A. *J. Chem. Phys.* **1972**, *56*, 2257. (b) Hariharan, P. C.; Pople, J. A. *Theor. Chim. Acta* **1973**, *28*, 213.

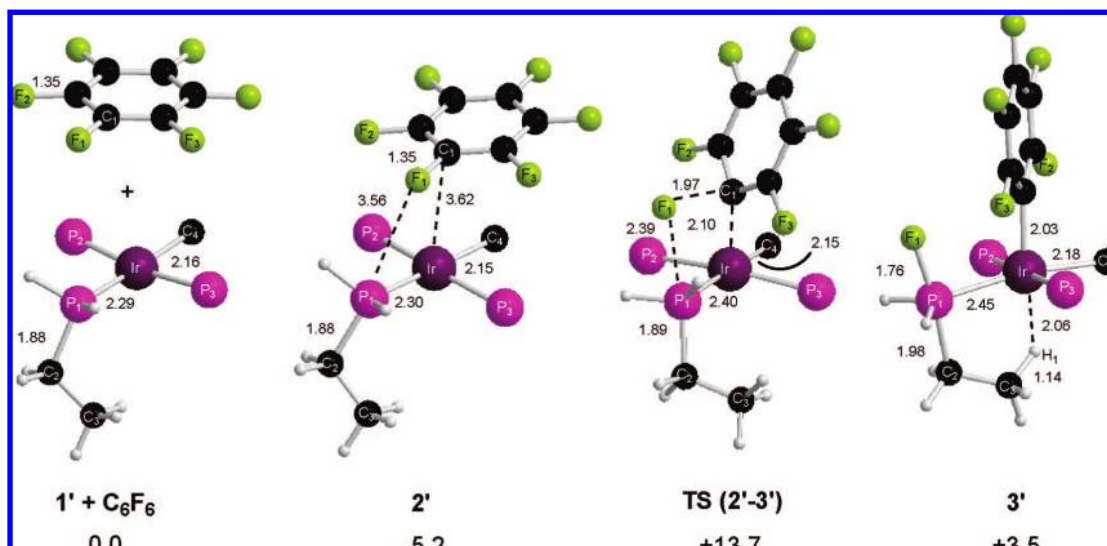


Figure 1. Computed geometries (with selected key distances in Å) and energies (kcal/mol) for stationary points along Pathway 1 (phosphine-assisted C–F activation). H atoms on the PH_3 and CH_3 ligands are omitted for clarity.

the following section. It should be noted that in the original report of the formation of **5**, a mechanism based on the initial cyclometalation of one PEt_3 ligand followed by single electron transfer to C_6F_6 was proposed.¹³ However, test calculations using model species **1'** showed this to be a very high-energy process, and so we have ruled out this possibility.²⁶

Pathway 1: Phosphine-Assisted C–F Activation. The computed geometries and relative energies of the stationary points involved in this process are shown in Figure 1. Initially, a loosely bound adduct is formed (**2'**, $E = -5.2$ kcal/mol) in which the geometries of **1'** and C_6F_6 are barely perturbed from their isolated structures. The C_6F_6 ring in **2'** lies roughly parallel to the metal coordination plane and a linear transit based on the shortest $\text{Ir}\cdots\text{C}$ contact allowed the location of a 4-centered transition state for phosphine-assisted C–F activation (**TS (2'–3')**, $E = +13.7$ kcal/mol) in which Ir, P1, F1, and C1 all participate. **TS (2'–3')** exhibits a very late geometry in terms of both the short $\text{Ir}\cdots\text{C1}$ distance (2.10 Å) and the upright orientation of the C_6F_5 moiety, which is close to that expected for a σ -aryl ligand. Significant elongation of the breaking $\text{C1}\cdots\text{F1}$ bond to 1.97 Å is also computed, and as anticipated as F1 moves out of the plane of the arene ring, it is directed toward the PH_2Et ligand ($\text{P1}\cdots\text{F1} = 2.39$ Å). The C–F and Ir–P bonds participating in this process are not coplanar ($\text{P1–Ir–C1–F1} = 34.5^\circ$), and this appears to be driven by maximizing any possible $\text{F}\cdots\text{P}$ interactions. In particular, F1 is positioned in an axial site in terms of the incipient 5-coordinate phosphorus center ($\text{F1–P1–Ir–C2} = 180.0^\circ$). In addition, similar orientations of the ortho fluorines relative to the two PH_3 ligands are seen, with short $\text{F2}\cdots\text{P2}$ and $\text{F3}\cdots\text{P3}$ contacts below 2.9 Å.

TS (2'–3') was found to link to the metallophosphorane intermediate, **3'** ($E = +3.5$ kcal/mol), which formally contains

a $[\text{PEtFH}_2]^-$ phosphoranide ligand with an Ir–P distance of 2.45 Å. **3'** exhibits a square-pyramidal geometry at Ir with an axial C_6F_5 ligand. The short computed Ir– C_6F_5 distance of 2.03 Å reflects the absence of a trans ligand, although an $\text{Ir}\cdots\text{H1}$ contact of 2.06 Å along with the elongation of the C3–H1 bond to 1.14 Å indicates an agostic interaction with the ethyl group of the phosphoranide ligand. Overall, relative to the isolated reactants the barrier associated with phosphine-assisted C–F activation along Pathway 1 is 13.7 kcal/mol.

Pathway 2: Oxidative Addition of C_6F_6 . This process can occur directly at 4-coordinate **1'** (Pathway 2a) or may be preceded by phosphine dissociation from **1'** to generate 3-coordinate $[\text{IrMe}(\text{PR}_3)_2]$ species (Pathway 2b). For Pathway 2b, phosphine loss may occur either cis or trans to Me, and overall, reaction via the latter was found to be more favorable and so will be discussed here.²⁷

Along Pathway 2a, direct oxidative addition to **1'** proceeds through the same precursor adduct **2'** located along Pathway 1. C–F bond activation then occurs via **TS (2'–6')**, ($E = +29.2$ kcal/mol, see Figure 2) with the methyl and PH_2Et ligands bending back to accommodate the approaching C_6F_6 substrate ($\text{C4–Ir–P1} = 122^\circ$). The C1–F1 bond is stretched to 1.56 Å in **TS (2'–6')** and is twisted relative to the C4–Ir–P1 plane by 26° . A coplanar arrangement would be more usual for a concerted oxidative addition process, and the computed distortion again seems to be driven by additional $\text{F}(\text{ortho})\cdots\text{P}$ interactions involving the PH_3 ligands ($\text{F2}\cdots\text{P2}$ and $\text{F3}\cdots\text{P3}$ both < 2.8 Å). The Ir^{III} –fluoride species formed, **6a'**, has the fluoride ligand trans to methyl and has a computed relative energy of -32.1 kcal/mol.

For Pathway 2b removal of the PH_2Et ligand trans to Me in **2'** results in its substitution by C_6F_6 and the formation of a new adduct, **trans-7'** ($E = +31.3$ kcal/mol). This process appears to be purely dissociative in nature, as scans based on the Ir–P1

(26) The barrier to cyclometallation of the PH_2Et ligand in **1'** is 36.4 kcal/mol, whereas the subsequent electron transfer to form separated radicals incurs a further +145.0 kcal/mol in the gas phase. Solvation effects, incorporated through the PCM approach (C_6F_6 , $e = 2.25$), reduce this value, but it remains prohibitively high at 97.4 kcal/mol. Initial electron transfer from **1'** to C_6F_6 was also tested and also found to be a high-energy process ($\Delta E = +150.1$ kcal/mol in the gas phase, dropping to 101.8 kcal/mol in benzene).

(27) *cis*- $\text{PH}_3/\text{C}_6\text{F}_6$ substitution in **1'** to form *cis*-**7'** ($E = +29.7$ kcal/mol) is in fact slightly more favorable than that of *trans*- $\text{PH}_2\text{Et}/\text{C}_6\text{F}_6$ substitution to form *trans*-**7'** ($E = +31.3$ kcal/mol). However, C–F activation in *cis*-**7'** then has a barrier of 4.1 kcal/mol, whereas C–F activation in *trans*-**7'** is effectively barrierless. Overall C–F activation is therefore easier via *trans*-**7'**. Details of the pathway via *cis*-**7'** are in the Supporting Information.

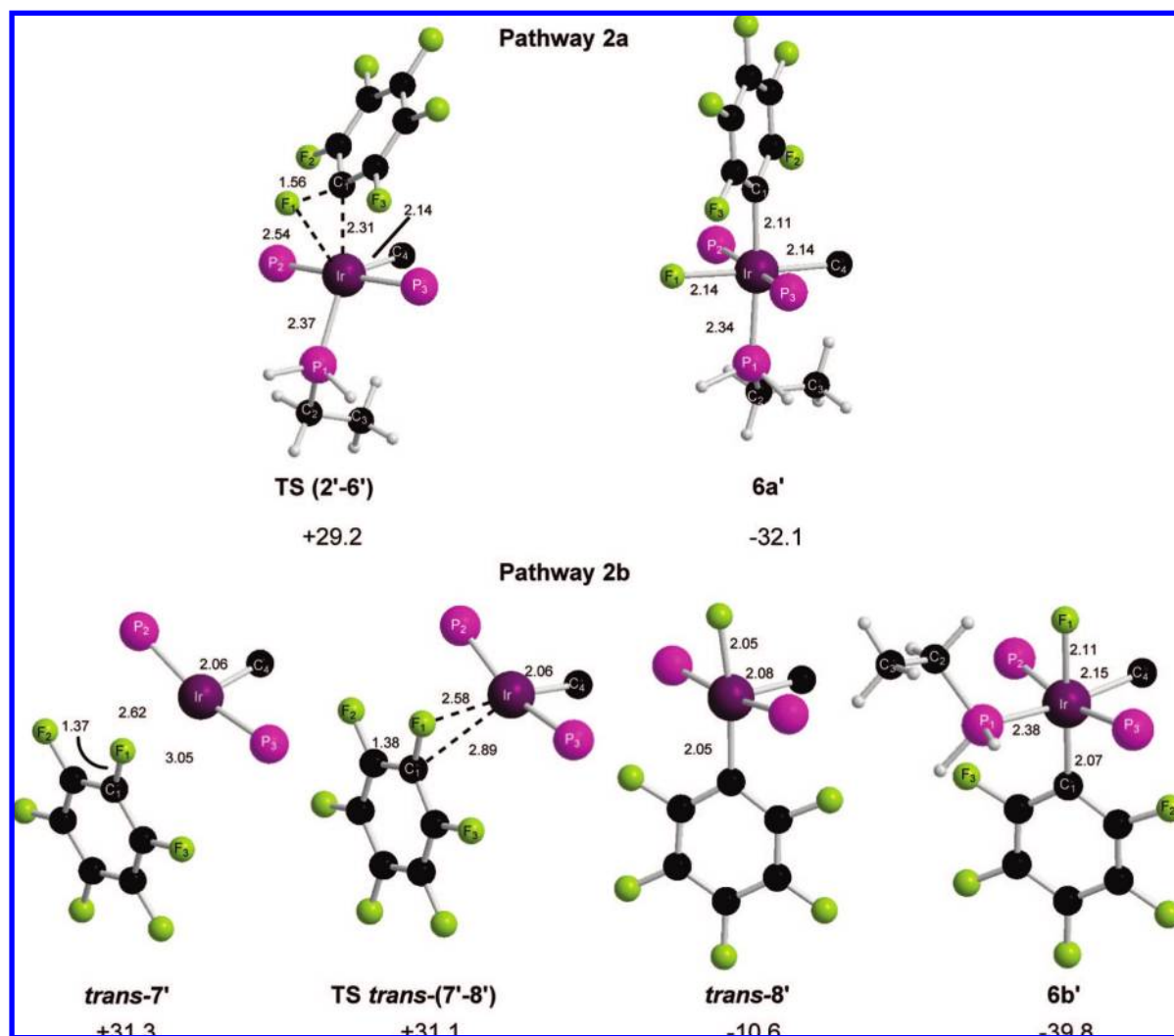


Figure 2. Computed geometries (with selected key distances in Å) and energies (kcal/mol) for stationary points along Pathways 2a and 2b (C–F oxidative addition). H atoms on the PH₃ and CH₃ ligands are omitted for clarity.

distance in **2'** showed no evidence for the approach of C₆F₆ toward the metal center until the phosphine ligand had effectively been completely removed from the metal. **trans-7'** exhibits shorter Ir···C1/F1 contacts than those in **2'**, although the C1–F1 bond length is only slightly elongated (1.37 Å). The energy surface around **trans-7'** is exceedingly flat, and concerted oxidative addition proceeds without any effective barrier to give 5-coordinate, square-pyramidal [Ir(C₆F₅)(F)(Me)(PH₃)₂], **trans-8'** ($E = -10.6$ kcal/mol) in which F1 has moved trans to C₆F₅ to leave Me in the axial position. Addition of PH₂Et therefore generates **6b'** ($E = -39.8$ kcal/mol), in which the F and PH₂Et ligands are swapped relative to **6a'**.

The energetics of the different C–F activation processes are summarized in Figure 3. All processes stem from the common adduct, **2'**, and the lowest lying C–F activation transition state is **TS (2'–3')** corresponding to the phosphine-assisted process (Pathway 1, $E = +13.7$ kcal/mol). The concerted oxidative addition processes have higher lying transition states, either at 4-coordinate Ir (Pathway 2a, **TS (2'–6')**, $E = +29.2$ kcal/mol) or at 3-coordinate Ir (Pathway 2b, **TS trans-(7'–8')**, $E = +31.1$ kcal/mol). To assess these pathways fully it is also necessary to consider the associated computed free energies (in italics, Figure 3). Entropy tends to disfavor both reactions proceeding directly from adduct **2'**, and Pathway 2a in particular has a very

high barrier of +43.8 kcal/mol and so can be ruled out as a possible mechanism. Overall Pathway 1, phosphine-assisted C–F activation, is computed to be the most accessible process ($\Delta G^\ddagger = +29.0$ kcal/mol), although Pathway 2b is only slightly less accessible ($\Delta G^\ddagger = +31.4$ kcal/mol).

The similar free energies of the transition states along Pathways 1 and 2b make it difficult to distinguish these two mechanisms on this basis alone. Further evidence for Pathway 1, however, can be found by considering the experimental selectivities reported by Milstein and co-workers in their original study.¹³ In particular, at 60 °C **1** was seen to react only with C₆F₆, and no reaction occurred with C₆H₆, C₆H₅F, or 1,3,5-C₆F₃H₃. The computed free energy barriers to C–H activation for C₆H₆ and 1,3,5-C₆F₃H₃ via Pathway 2b are 28.9 and 27.2 kcal/mol, respectively, both somewhat lower than the equivalent barriers for C–F activation of C₆F₆ via either Pathway 1 or 2b. Therefore, if Pathway 2b were operative, C–H activation of C₆H₆ and 1,3,5-C₆F₃H₃ would be expected under the conditions utilized for the C₆F₆ reaction. As this is not the case, another mechanism must be operative. We believe this to be the

(28) C–H activation of benzene via a phosphine-assisted C–H activation process was found to be extremely unfavorable, the metallaphosphorane intermediate formed, [Ir(PH₃)₂(Me)(Ph)(PH₃Et)], having a prohibitively high energy of +56.1 kcal/mol.

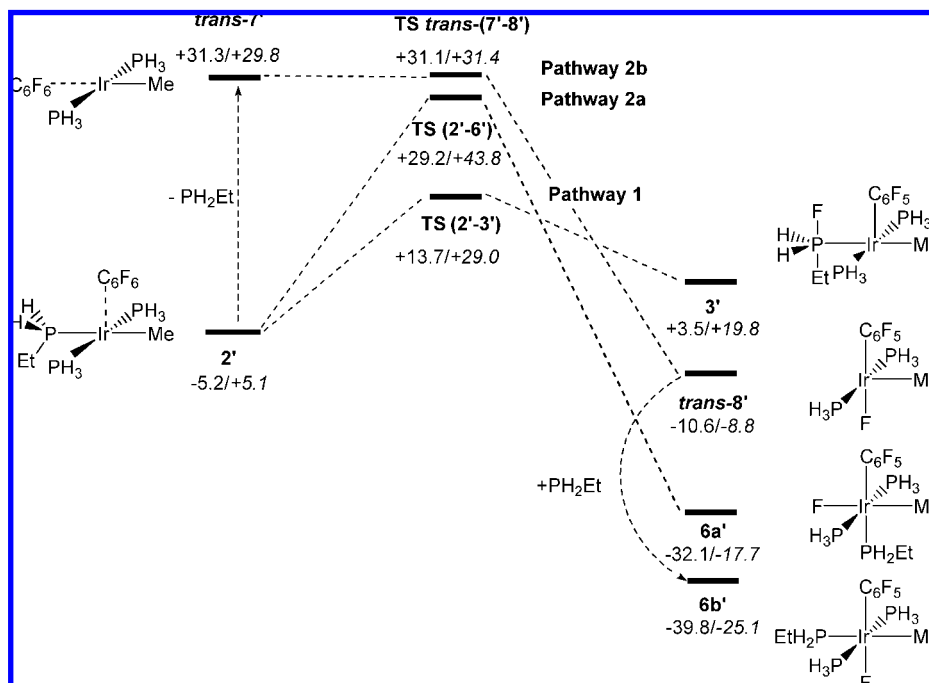


Figure 3. Computed reaction profiles (kcal/mol) for Pathway 1 (phosphine-assisted C–F activation) and Pathways 2a and 2b (C–F oxidative addition). Free energies are given in italics.

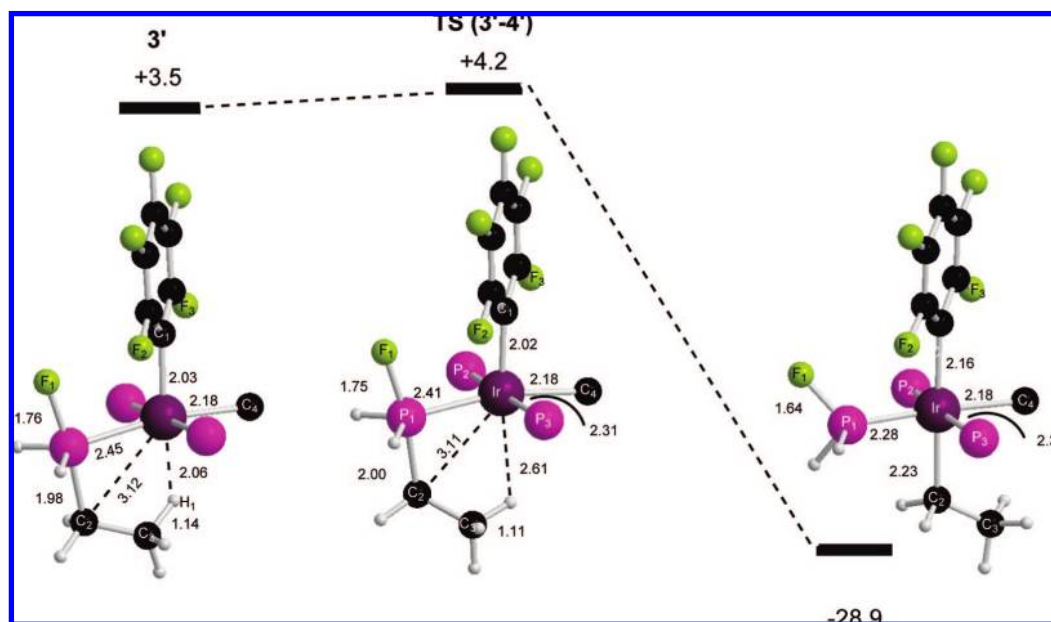


Figure 4. Computed geometries (with selected key distances in Å) and energies (kcal/mol) for ethyl transfer from 3' to give 4'. H atoms are omitted from PH₃ and CH₃ ligands for clarity.

phosphine-assisted C–F activation process, and we go on to show below that this mechanism is indeed consistent with the greater reactivity of C₆F₆ compared to that of lesser fluorinated arenes.^{28,29}

Formation of *trans*-[Ir(C₆F₅)(PH₃)₂(PH₂F)] (*trans*-5') from 3'. On the basis of the above discussion we assume in the following that C–F activation proceeds via Pathway 1 to give the metallophosphorane intermediate 3'. The geometry of this species is ideally set up for ethyl group transfer from the phosphoranide ligand to iridium to generate 4', and this occurs with a minimal activation energy of +0.7 kcal/mol via TS

(3'–4') (see Figure 4). In forming TS (3'–4'), the major motion is a rotation about the P–Et bond that disrupts the agostic interaction in 3' and makes a vacant site at the metal available to accept the ethyl moiety. Apart from this, a slight elongation of the P1–C2 distance and a concomitant shortening of the

(29) An additional feature of the experimental selectivity was that C–H activation (but *not* C–F activation) was seen at 80 °C. Our calculations for 1,3,5-C₆F₃H₃ via Pathway 2b reproduce this preference with C–H activation ($\Delta G^\ddagger = +27.2$ kcal/mol) being far more accessible than C–F activation ($\Delta G^\ddagger = +37.9$ kcal/mol). It may be that at higher temperatures phosphine ligand dissociation becomes possible and so makes oxidative addition via Pathway 2b accessible.

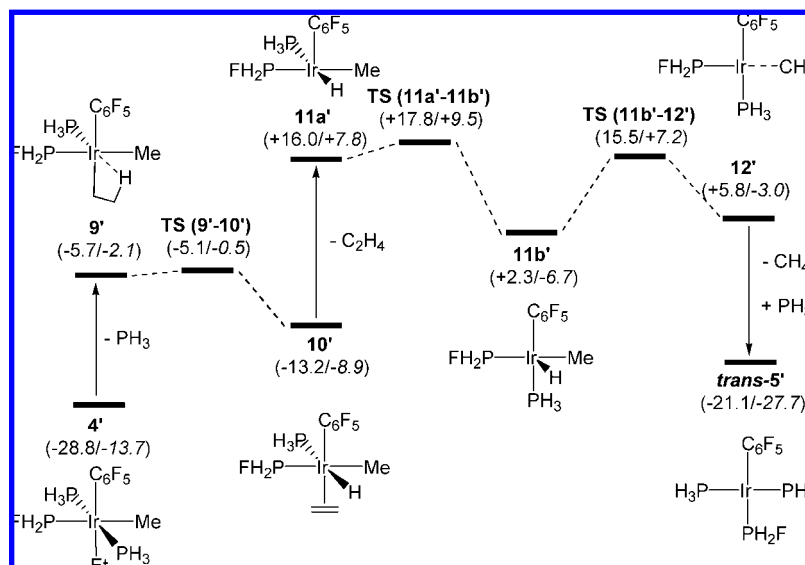


Figure 5. Computed reaction profile (kcal/mol) for the formation of the final model product *trans*-[Ir(C₆F₅)(PH₃)₂(PH₂F)] (*trans*-5') from the fluorophosphine ethyl intermediate 4'. Free energies are given in italics.

P1–F1 bond are computed. The species formed is pseudo-octahedral 4' ($E = -28.9$ kcal/mol) in which the C₆F₅ ligand is *trans* to ethyl and the Ir–C₆F₅ distance has lengthened accordingly to 2.16 Å. Comparing the structures of 3' and 4' shows the Ir–P1 bond shortens significantly upon Et group transfer. This is consistent with other computational studies that show metal–phosphorane (M–PR₄) bonds to be longer than equivalent metal–phosphine (M–PR₃) bonds.^{15,22e,30} Experimentally, there are two examples where the transformation of an M–PR₄ moiety into a M–PR₃/R species has been directly observed,^{22c,d} although unfortunately, in neither case are structural data of both species available for comparison.

The formation of the model product, *trans*-[Ir(C₆F₅)(PH₃)₂(PH₂F)] (*trans*-5'), from 4' requires the β-H elimination of ethene and the reductive elimination of methane. Both steps present several mechanistic possibilities in terms of the isomers involved, or for reductive elimination, different metal coordination numbers, and we shall present only one such possible pathway here, as summarized schematically in Figure 5. The computed geometries of the stationary points involved are rather standard and are supplied in the Supporting Information. Starting from 4', dissociation of a PH₃ ligand permits formation of an agostic complex, 9' ($E = -5.7$ kcal/mol) from which β-H transfer occurs with a small activation barrier of +0.6 kcal/mol to give the hydrido-alkene complex 10' ($E = -13.2$ kcal/mol). Experimentally, reductive elimination from octahedral Ir(III) complexes is thought to occur after initial ligand loss,³¹ and so we have assumed ethene dissociation occurs at this stage to produce 5-coordinate square-pyramidal 11a' featuring an axial C₆F₅ ligand. We found that prior to reductive elimination a facile isomerization to an H-axial form was necessary (11b', $E = +2.3$ kcal/mol). Reductive elimination then proceeds with a barrier of +13.2 kcal/mol to give the methane σ-complex 12'. CH₄/PH₃ substitution yields the final product *trans*-5'. The alternative isomer, *cis*-5', was found to be 1.1 kcal/mol higher in energy,

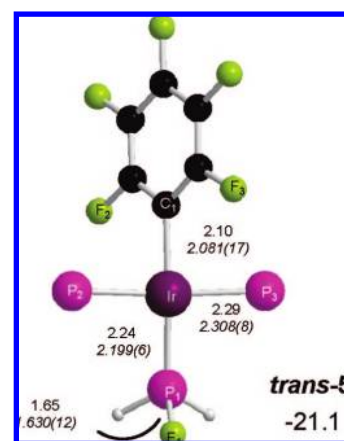


Figure 6. Computed structure of *trans*-5' with selected key computed and (in italics) experimental¹² distances in Å. For the Ir–P₂/P₃ bond the average distance determined experimentally is indicated.

consistent with the fact that the *trans*-isomer of 5 is seen experimentally. The computed geometry of *trans*-5' compares well with that determined experimentally for *trans*-5 with, in particular, a shorter M–P bond being computed to the fluorophosphine, due to the greater π-acceptor capacity of that ligand (see Figure 6).

The computed reaction profile in Figure 5 shows that the major barriers to the formation of *trans*-5' from 4' involve ligand dissociation, although in each case the favorable entropy contribution reduces the free energy barriers (in italics). In terms of the overall reaction from 1' the highest point along the reaction profile is TS (2'–3') ($G = +29.0$ kcal/mol), and this step also has the largest individual free energy barrier (+23.9 kcal/mol relative to 2'). The final products, *trans*-5' plus free C₂H₄ and CH₄, are also the most stable species along the profile ($G = -27.7$ kcal/mol).

Characterization of Phosphine-Assisted C–F Activation. We have formulated this process in terms of the nucleophilic attack of an electron-rich Ir(I) metal center at an electron-deficient C₆F₅ substrate. This view accounts for the selectivities seen experimentally, where no reaction was seen with lesser fluorinated

(30) Brown, D. A.; Deignan, J. P.; Fitzpatrick, N. J.; Fitzpatrick, G. M.; Glass, W. K. *Organometallics* **2001**, *20*, 1636.

(31) Driver, M. S.; Hartwig, J. F. *Organometallics* **1998**, *17*, 1134. references therein.

substrates such as C_6H_5F or 1,3,5- $C_6H_3F_3$ or with the less nucleophilic metal complex $[IrCl(PEt_3)_3]$.¹² To assess the role of the metal environment on phosphine-assisted C–F activation the barriers for the reactions of C_6F_6 with *trans*- $[IrMe(PMe_3)_2(PMe_2Et)]$, **1'(PMe₃)**,³² and *trans*- $[IrCl(PH_3)_2(PH_2Et)]$, **1'(Cl)** have been computed. In both cases computed geometries involved were very similar to those located with **1'**. The introduction of methyl groups on the phosphines in **1'(PMe₃)** reduces the activation barrier to only 10.4 kcal/mol,³³ consistent with the more electron-releasing trialkylphosphines creating a more nucleophilic metal center.³⁴ Conversely, the computed activation barrier with **1'(Cl)** increases to 15.6 kcal/mol due to the electron-withdrawing effect of the Cl ligand. In addition, the energy of the metal-centered d_{z^2} HOMO in these complexes are found to increase along the series **1'(Cl)** (−4.41 eV) < **1'** (−3.97 eV) < **1'(PMe₃)** (−3.24 eV). As it is this orbital that supplies the electrons for nucleophilic attack, the correlation between a higher HOMO energy and a lower activation barrier supports our view of this reaction.

We have also computed the barrier to phosphine-assisted C–F bond activation at **1'** for a range of fluoroarene substrates (**I–VI**, see Figure 7). For substrates **II**, **IIIa**, and **IVa** very similar geometries to those shown above for **2'** and **TS (2'–3')** were located. In contrast, for **IVb**, **Vb/c**, and **VI** the precomplexes exhibit a perpendicular orientation of the substrate with one C–H bond pointing directly at the metal center. The transition state geometries for these species are also different in that the closest F1···P distance is typically about 2.5 Å and involves

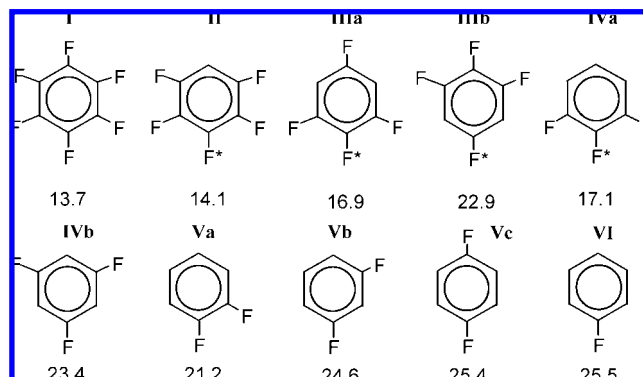


Figure 7. Computed activation energies (kcal/mol) for phosphine-assisted C–F activation of fluoroarenes by **1'**. Barriers are quoted relative to the isolated reactants set to zero, and where necessary, the activating C–F bond is denoted with an asterisk.

one of the PH_3 ligands rather than PH_2Et . The $Ir\cdots Cl$ and $Cl\cdots F1$ distances are relatively unaffected by this change in orientation, however, IRC calculations do indicate that C–F activation occurs with F transfer onto a PH_3 ligand. This different behavior appears to be linked to the loss of the 1,2,3-trifluoro substitution pattern in these substrates, possibly because this arrangement allows a network of weak ortho- $F\cdots PH_3$ interactions to be established that stabilizes the parallel orientation of the substrate in the precomplex. Such interactions were noted above in **TS (2'–3')** and seem to play a role in directing the transferring fluorine to the PH_2Et ligand in the transition state.³⁵ For 1,2- $C_6F_4H_2$ (**Va**) an intermediate situation is seen in the precomplex in which the substrate is tilted by ca. 45° with respect to the metal coordination plane. In this case phosphine-assisted C–F activation again transfers fluorine onto a *cis*- PH_3 ligand.

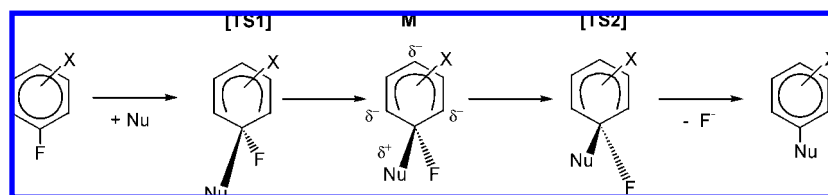
Figure 7 shows that, of the processes considered, the reaction of C_6F_6 entails the lowest activation energy. Moreover, this is 10–12 kcal/mol lower than 1,3,5- $C_6F_3H_3$ and C_6H_5F , consistent with the fact that of these three species only C_6F_6 undergoes C–F bond activation at **1** at 60 °C. More generally, the computed activation energy is sensitive to the pattern of fluorine substitution, and the largest effect is associated with the number of F-substituents ortho to the C–F bond being broken. Comparing **I** vs **IIIb**, **II** vs **IVb** and the **IVa/Va/VI** series suggests that each ortho-H/F substitution lowers the barrier to phosphine-assisted C–F activation by ~4 kcal/mol. H/F substitution in a meta position also has a stabilizing effect on the transition state, albeit somewhat smaller (~1–1.5 kcal/mol per F—see **I** vs **IIIa**, **II** vs **IVa** and the **IVb/Vb/VI** series). para-H/F substitution has only a minor stabilizing effect (**I** vs **II**, **IIIa** vs **IVa**, and **Vc** vs **VI**).

Our computational results can be compared with those obtained experimentally for the S_NAr reactions of $C_6F_{6-n}H_n$ ($n = 0–2$) species with $NaOMe$ ³⁶ and the organometallic nucleophile $[CpFe(CO)_2]^-$.^{10a,b} Both systems display similar reactivity patterns, and with $NaOMe$ rate constants indicate that H/F substitution either meta or ortho accelerates the reaction, with

- (32) Calculations were attempted on the full species **1**, but difficulties were encountered with locating true minima due to the large number of soft modes corresponding to ethyl group rotations.
- (33) Another difference found with the **1'(PMe₃)** model was the presence of a second intermediate ($E = -0.1$ kcal/mol) between the normal precomplex **2'** ($E = -4.6$ kcal/mol) and the C–F activation transition state. However, the transition state linking these two pre-complexes is low in energy ($E = +0.1$ kcal/mol), and so the overall barrier still corresponds to the C–F activation step.
- (34) We also computed the energetics for Pathways 2a and 2b starting from the model species **1'(PMe₃)**. All attempts to locate a transition state analogous to **TS (2'–6')** for direct oxidative addition failed and led instead to the much more stable phosphine-assisted transition state at +10.4 kcal/mol. For Pathway 2b dissociation of the PMe_2Et ligand from **1'(PMe₃)** (+28.7 kcal/mol) is in fact significantly easier than PH_2Et dissociation from **1'** (+37.4 kcal/mol). This stabilisation of about 9 kcal/mol is retained in the subsequent C_6F_6 adduct ($E = +22.5$ kcal/mol) and the C–F activation transition state ($E = +22.5$ kcal/mol) derived from **1'(PMe₃)**. Changing from **1'** to **1'(PMe₃)** therefore affects the energy of phosphine dissociation but not of the actual C–F oxidative addition step, which is effectively barrierless with both models. Most importantly the activation enthalpy associated with Pathway 2b from **1'(PMe₃)** is more than 12 kcal/mol above that for Pathway 1, phosphine-assisted C–F activation ($E = +10.4$ kcal/mol). Inclusion of entropic effects does result in a reversal of this preference; however, we believe the computed entropy of phosphine dissociation is significantly overestimated in the current calculations. A similar situation is seen for the cyclometalation reaction of $[Ir(CH_2CMe_3)PMe_3]_3$ ^{34a} which has been shown experimentally to proceed without initial PMe_3 dissociation.^{34b} Computed enthalpies on the full experimental system for this process favor direct C–H activation ($\Delta E = +18.2$ kcal/mol cf. +25.9 kcal/mol for the alternative process with initial PMe_3 loss). However, a very large ΔS^\ddagger value of +48.2 cal·mol⁻¹·K⁻¹ for the dissociative route (arising almost entirely from PMe_3 loss) reverses the order, and the computed free energies of +19.2 kcal/mol (cf. only +11.6 kcal/mol for the dissociative mechanism) predict the latter would be preferred. The situation—and the nature of the Ir complex involved—are very similar to the $[IrMe(PMe_3)_3]$ model system under consideration here, but for $[Ir(CH_2CMe_3)(PMe_3)_3]$ cyclometalation comparison with experiment gives a clear indication that the entropic contribution associated with phosphine loss is overestimated. (a) Tulip, T. H.; Thorn, D. L. *J. Am. Chem. Soc.* **1981**, *103*, 2448. (b) Harper, T. G. P.; Desrosiers, P. J.; Flood, T. C. *Organometallics* **1990**, *9*, 2523.

- (35) This feature is retained with **1'(PMe₃)**, even though the increased steric bulk of the PMe_3 ligands causes the $F(\text{ortho})\cdots P$ contacts to increase to about 2.95 Å. The fact that, when this pattern is absent, F1 transfers onto PH_3 rather than PH_2Et does reflect the make-up of our model system; however, this result is entirely consistent with the build-up of negative charge on F1 in the transition state (see below), and the movement of this nucleophilic species towards the less electron-rich (non-alkyl) phosphine.

Scheme 3



the introduction of meta-F substituents having the greater effect. These trends have been interpreted in terms of the classical picture of an S_NAr reaction which is usually considered to proceed in two steps via a cyclohexadienyl (or Meisenheimer) complex (**M**, see Scheme 3).³⁷ When the leaving group is a halide the first step via **TS1** is thought to be rate determining. The faster reactions seen with meta-F substituted species compared to their para- or ortho-substituted analogues have been explained in terms of the π -donor capacity of F. This leads to repulsive interactions with arene ring π -system, an effect that is accentuated at the ortho and para sites due to the build up of negative charge in **TS1** and **M**. A meta-F substituent avoids this destabilizing effect. The situation is not clear, however, as this analysis would suggest a similar effect for ortho and para substitution.^{36a,b} The strong σ -withdrawing effect of ortho-F substituents and the creation of a highly electrophilic ipso-carbon have therefore been invoked to explain experimental trends.^{36c}

The phosphine-assisted C–F activation process considered here, however, deviates from this classical picture, most obviously as it is a one-step process. Moreover, in all cases the computed C–F activation transition state geometry exhibits a short Ir–C1 distance of around 2.1 Å and a long C1...F1 distance in excess of 1.9 Å, indicative of a very late transition state more akin to **TS2** in Scheme 3. An analysis of the computed natural atomic charges along the reaction profile supports this view. In particular, the predicted distribution of negative charge to the ortho and para sites around the arene ring upon going from precomplex **2'** to the 4-centered **TS** (**2'–3'**) is not seen.³⁸ Instead, significant changes in charge occur only at Ir (+0.45e), C1 (–0.35e), and F1 (–0.23e), and the charges in the transition state are much more similar to those of **3'**, the initial product of C–F bond activation (see Figure 8 for C_6F_6). Similar changes in charge distribution were found for all the substrates considered including the least fluorinated substrate, C_6H_5F , where the changes at the key atomic centers between **2'** and **TS(2'–3')** were Ir (+0.38e), C1 (–0.32e), and F1 (–0.19e).

The late transition state geometries involved in phosphine-assisted C–F activation suggest that a major factor that will determine the activation barrier should be the strength of the new Ir–aryl bond that is being formed. In this context it is interesting to note the results of recent computational studies on $CpRe(CO)_2(C_6F_nH_{5-n})(H)$ species which show that the Re–aryl bond strength increases significantly with the number of

ortho-F substituents that are present.³⁹ A similar effect appears to be in play here.⁴⁰

Conclusions

Density functional calculations have been used to model possible mechanisms for the unusual C–F bond activation reaction between C_6F_6 and $[IrMe(PEt_3)_3]$. A novel mechanism, phosphine-assisted C–F activation, has been characterized which involves nucleophilic attack of the electron-rich organometallic and trapping of the displaced fluoride by a phosphine ligand to form a metallophosphorane intermediate; effectively C–F activation proceeds by a 1,2 addition over the Ir–P bond. Although ultimately acting as fluoride acceptors, strongly electron-donating phosphines may be required to make the metal center sufficiently nucleophilic to promote the phosphine-assisted C–F activation process. Once formed the metallophosphorane readily transfers an ethyl group to the metal center, and subsequent β -H elimination of ethene and reductive elimination of methane then fully account for the observed products. This phosphine-assisted C–F activation mechanism proceeds via a 4-centered transition state and involves relatively late transition state geometries, the energies of which are determined by the strength of the new M–aryl bond that is being formed. The presence of ortho-F substituents in particular promotes the reaction. Phosphine-assisted C–F activation represents a further mechanistic possibility for the activation of C–F bonds by transition metals and may be important for electron-rich metal centers bearing phosphine ligands. As we shall show in the accompanying paper²¹ these conditions can also be met by *bis*-trialkylphosphine Pt(0) complexes.

Acknowledgment. We thank Dr. Vladimir V. Grushin (Dupont, Wilmington), Prof. Robin N. Perutz (University of York) and Prof. John E. McGrady (University of Glasgow) for useful discussions. The support of the EPSRC for a postdoctoral fellowship (SE) through grant number GR/T28539/01 is gratefully acknowledged.

Supporting Information Available: Cartesian coordinates and energies of all computed species; full reference 23. This material is available free of charge via the Internet at <http://pubs.acs.org>.

JA804622J

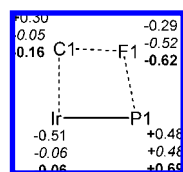


Figure 8. Computed natural atomic changes for precomplex **2'** (plain text), **TS** (**2'–3'**) (italics), and metallophosphorane intermediate **3'** (bold) for the reaction of C_6F_6 with *trans*-**1'**.

- (36) (a) Burdon, J.; Hollyhead, W. B.; Patrick, C. R.; Wilson, K. V. *J. Chem. Soc.* **1965**, 6375. (b) Burdon, J.; Hollyhead, W. B. *J. Chem. Soc.* **1965**, 6326. (c) Chambers, R. D.; Close, D.; Williams, D. L. H. *J. Chem. Soc., Perkin Trans. 2* **1980**, 778.
- (37) (a) Miller, J. *Aromatic Nucleophilic Substitution*; Elsevier: Amsterdam, 1968. (b) Dillow, G. W.; Kebarle, P. *J. Am. Chem. Soc.* **1988**, *110*, 4877.
- (38) The largest increase in negative charge was usually about 0.03e and was located at an ortho carbon site.
- (39) Clot, E.; Besora, M.; Maseras, F.; Mégret, C.; Eisenstein, O.; Oelckers, B.; Perutz, R. N. *Chem. Commun.* **2003**, 490.
- (40) The dominance of ortho-F substituents (over meta) in determining the selectivity of S_NAr processes has also been noted for the reactions of fluoropyridines with NaOMe.^{36c}